Minority carrier lifetime of lattice-matched CdZnTe alloy grown on InSb substrates using molecular beam epitaxy

Shi Liu, Xin-Hao Zhao, Calli Campbell, Michael J. DiNezza, Yuan Zhao, and Yong-Hang Zhang

Articles you may be interested in

Determination of CdTe bulk carrier lifetime and interface recombination velocity of CdTe/MgCdTe double heterostructures grown by molecular beam epitaxy
Appl. Phys. Lett. **105**, 252101 (2014); 10.1063/1.4904993

Impact of dislocations on minority carrier electron and hole lifetimes in GaAs grown on metamorphic SiGe substrates
Appl. Phys. Lett. **84**, 3447 (2004); 10.1063/1.1736318

Effect of dislocations on minority carrier lifetime in HgCdTe
J. Appl. Phys. **95**, 2467 (2004); 10.1063/1.1644039

Radiative and nonradiative recombination processes in lattice-matched (Cd,Zn)O/(Mg,Zn)O multiquantum wells
Appl. Phys. Lett. **77**, 1632 (2000); 10.1063/1.1308540

N -type doping of lattice-matched ZnCdSe and Zn x Cd y Mg 1−x−y Se epilayers on InP using ZnCl 2
J. Appl. Phys. **84**, 1472 (1998); 10.1063/1.368210

Minority carrier lifetime of lattice-matched CdZnTe alloy grown on InSb substrates using molecular beam epitaxy

Shi Liu
Center for Photonics Innovation and School of Electrical, Computer and Energy Engineering, Arizona State University, Tempe, Arizona 85287

Xin-Hao Zhao and Calli Campbell
Center for Photonics Innovation and School for Engineering of Matter, Transport and Energy, Arizona State University, Tempe, Arizona 85287

Michael J. DiNezza, Yuan Zhao, and Yong-Hang Zhang[a]
Center for Photonics Innovation and School of Electrical, Computer and Energy Engineering, Arizona State University, Tempe, Arizona 85287

A CdZnTe/MgCdTe double-heterostructure (DH) consisting of a 3 μm thick $Cd_{0.9946}Zn_{0.0054}Te$ middle layer that is lattice-matched to an InSb substrate has been grown using molecular beam epitaxy. A long carrier lifetime of 3.4×10^2 ns has been demonstrated at room temperature, which is approximately three times as long as that of a CdTe/MgCdTe DH with identical layer thickness. This substantial improvement is due to the reduction in misfit dislocation density in the CdZnTe alloy. In contrast, a CdTe/MgCdTe DH with 3 μm thick CdTe layer grown on an InSb substrate exhibits a strain relaxation of $\sim$30%, which leads to a wider x-ray diffraction peak, a weaker integrated photoluminescence intensity, and a shorter minority carrier lifetime of 1.0×10^2 ns. These findings indicate that CdZnTe lattice-matched to InSb has great potential as applied to high-efficiency solar cells as well as virtual substrates for high-performance large-area HgCdTe focal plane arrays. © 2015 American Vacuum Society. [http://dx.doi.org/10.1116/1.4905289]

I. INTRODUCTION

There has been growing interest in CdTe solar cells in recent years due to continuing improvements in device performance and market share. The efficiency record of polycrystalline CdTe solar cells has been frequently broken, recently reaching 21.0%.[1] However, this is still more than ten absolute percent lower than the Shockley–Queisser limit. Although the short-circuit current density is already close to the theoretical limit, there is still significant room for improvement in open-circuit voltage (V_{OC}) and fill factor, which are currently below 0.9 V and 80%, respectively, for most devices.[2] Such imperfections are believed to be due to large defect density, short minority carrier lifetime and so on. The use of monocrystalline CdTe is anticipated to improve the V_{OC} dramatically because of its better material quality and longer carrier lifetime. Several research efforts have demonstrated long carrier lifetimes in both epitaxial CdTe on InSb and bulk CdTe, along with a V_{OC} of greater than 0.9 V in monocrystalline CdTe solar cells.[3–9] Regardless of these new achievements, CdTe is not completely lattice-matched to InSb, which may cause material quality degradation when the CdTe epilayer is beyond a certain thickness (e.g., 2 μm). This problem can be circumvented by adding a small fraction of Zn into CdTe in order to form a CdZnTe alloy that is completely lattice-matched to InSb and exhibits a negligible increase in bandgap. A longer minority carrier lifetime is thus expected in the CdZnTe epilayer, especially when the layer is more than 2 μm thick,

since the misfit dislocation density is lower in this lattice-matched material system. Moreover, CdZnTe alloys grown on InSb, with tunable Zn compositions, can provide high-quality virtual substrates for HgCdTe growth. The advantages of this approach include: (1) CdZnTe is chemically compatible with, and lattice-matched to, HgCdTe;[10,11] (2) InSb substrates are of both high quality and low cost which overcomes the existing cost issues of CdZnTe substrates that impede their widespread application in large-area focal plane arrays;[10,11] and (3) CdZnTe on InSb offers better material quality compared to other alternative substrate techniques, such as CdTe/Si,[12] CdTe/Ge,[13] CdTe/GaAs,[14] CdTe/GaSb,[15] and InSb,[16] and thus has the feasibility to achieve high performance in long-wavelength infrared detectors.

II. EXPERIMENT

In this paper, we report the demonstration of a high-quality $Cd_{0.9946}Zn_{0.0054}Te/Mg_{0.24}Cd_{0.76}Te$ double-heterostructure (DH) grown on an InSb (100) substrate by molecular beam epitaxy (MBE) and characterized by high-resolution x-ray diffraction (XRD), steady-state photoluminescence (PL), and time-resolved photoluminescence (TRPL). Two sets of samples have been studied here. The first set consists of samples A to C (growth run numbers are A1654, A1656, and A1659, respectively), which are 1 μm CdZnTe layers grown under various Zn fluxes, for the purpose of lattice-match calibration. The second set consists of samples D and E (growth run numbers are A1667 and A1666, respectively), which are 3 μm CdTe/ $Mg_{0.24}Cd_{0.76}Te$ and $Cd_{0.9946}Zn_{0.0054}Te/Mg_{0.24}Cd_{0.76}Te$ DHs, for structural and optical properties comparisons. The

[a]Electronic mail: yhzhang@asu.edu

schematic layer structures of samples D and E are shown in Fig. 1. The 30 nm MgCdTe barrier layers, with Mg compositions of 24%, prevent photogenerated carriers from reaching the top surface and bottom buffer/substrate interface to recombine nonradiatively. The Zn composition in the CdZnTe alloy is designed to be 0.54% so that the alloy is perfectly lattice-matched to the InSb substrate.

All the samples are grown using a VG V80H dual-chamber MBE system with separate III-V and II-VI growth chambers connected by an ultrahigh vacuum (UHV) transfer chamber. The oxide removal process of InSb substrates starts with an initial substrate temperature ramp to a thermocouple reading of $500\,°C$ at $20\,°C/min$. Then, the temperature is further ramped up at a slower rate of $5\,°C/min$ in $5\,°C$ intervals, with a 3 min pause after each ramp to prevent the substrate from overheating, until a pyrometer reading of $475–480\,°C$ is reached. Such a careful temperature ramp is necessary because the InSb oxide removal temperature is very close to the InSb melting point. The substrates are kept at this temperature for one hour, and the completion of oxide removal is then indicated by streaky pseudo-(1×3) reflection high energy electron diffraction patterns. Next, the substrate temperature is brought down to $390\,°C$ for the 500 nm InSb buffer growth, with a growth rate of 9.1 nm/min and a Sb/In flux ratio of 1.5. After the III-V growth, the samples are transferred to the II-VI chamber under UHV, which avoids surface oxidation and contamination. The II-VI layers are grown at $265\,°C$ with a growth rate of 9.6 nm/min and a Cd/Te flux ratio of 1.5. Detailed growth procedures of II-VI layers can be found in the previous publication.[3]

III. RESULTS AND DISCUSSION

The lattice-match calibration of the CdZnTe alloy to the InSb substrate is carried out by measuring the XRD patterns of samples A to C and from there determining the Zn composition. The $\omega/2\theta$ scans at the (004) orientation of samples A to C, which are grown under Zn cell temperatures of 235, 245, and $255\,°C$, respectively, are shown in Fig. 2. It is observed that there are two separate peaks in samples A and B that correspond to the strained CdZnTe layer and the InSb
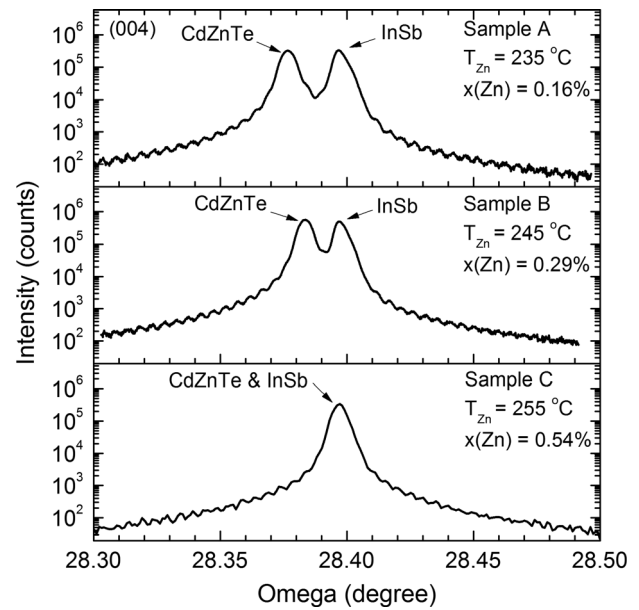

FIG. 1. Schematic layer structures of sample D: CdTe/$Mg_{0.24}Cd_{0.76}$Te DH, and sample E: $Cd_{0.9946}Zn_{0.0054}$Te/$Mg_{0.24}Cd_{0.76}$Te DH.
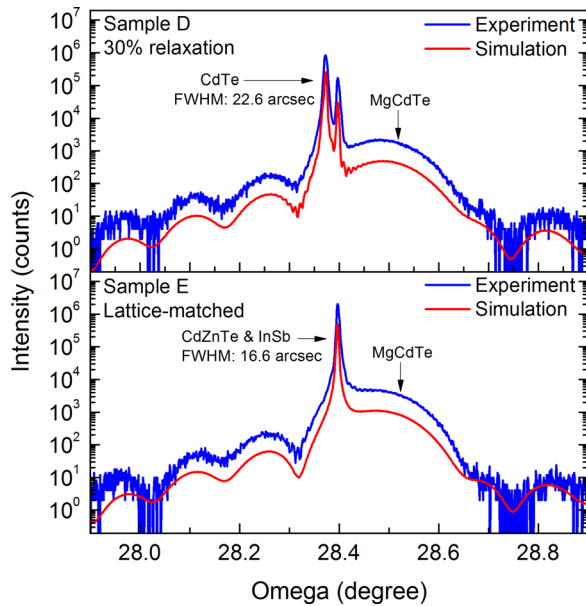
FIG. 2. High-resolution x-ray diffraction (004) patterns of samples A, B, and C, which have 1 μm CdZnTe layers on InSb substrates, showing that a complete lattice match is achieved.

substrate. However, in sample C, the two peaks merge together, indicating that a complete lattice match is reached. The Zn compositions listed in the figure are obtained by fitting the measured diffraction patterns based on the published structural parameters of ZnTe, CdTe,[17] and InSb. The narrow full-width at half-maximums (FWHMs) of the CdZnTe peaks, which are comparable to those of InSb substrates, along with the clear Pendellösung fringes are indicators of high quality CdZnTe layers and smooth CdZnTe/InSb interfaces. The (004) $\omega/2\theta$ scans are also performed for samples D and E, and the experimental and simulated diffraction patterns are shown in Fig. 3. The diffraction pattern of sample D clearly shows two separate peaks representing InSb and CdTe, and a strain relaxation of $\sim$30% for the CdTe layer is determined by XRD pattern simulation. In contrast, only one peak is present in the diffraction pattern of sample E, which means that the CdZnTe layer and the InSb substrate are lattice-matched. A larger FWHM of 22.6 arc sec observed for sample D compared to that for sample E (16.6 arc sec) shows degraded material quality due to strain relaxation. The broad peaks of the MgCdTe barrier layers and the Pendellösung fringes are observed in both samples, indicating the high material quality of these layers and smooth MgCdTe/Cd(Zn)Te interfaces.

The steady-state PL spectra of samples D and E are measured at room temperature using a 532 nm diode pumped solid state laser as a pumping source. The laser excitation power density is kept at 100 mW/cm^2 to mimic AM 1.5G solar radiation and to protect the II-VI layers from thermal damage by laser heating. As shown in Fig. 4, sample D has a PL peak wavelength of 825 nm, which corresponds to a band-to-band transition energy of 1.503 eV, while sample E has a PL peak wavelength of 824 nm, which corresponds to a band-to-band transition energy of 1.505 eV. Such a slight

FIG. 3. (Color online) High-resolution x-ray diffraction (004) patterns for samples D (3 μm CdTe/MgCdTe DH) and E (3 μm CdZnTe/MgCdTe DH). The 3 μm CdTe layer has a relaxation of ~30%, while the 3 μm CdZnTe layer is completely lattice-matched to the InSb substrate. They also clearly show that the CdTe peak has a FWHM of 22.6 arc sec, compared to the value of 16.6 arc sec for the CdZnTe peak, indicating that strain relaxation results in degraded material quality.

increase in the transition energy indicates that the bandgap increase caused by introducing 0.54% Zn in the CdTe binary is negligible. This is desirable for solar cells since any deviation from the optimal bandgap for single-junction solar cells should be avoided. The integrated PL intensity of sample E is at least one order of magnitude higher than that of sample D. Note that although the lattice mismatch between CdTe
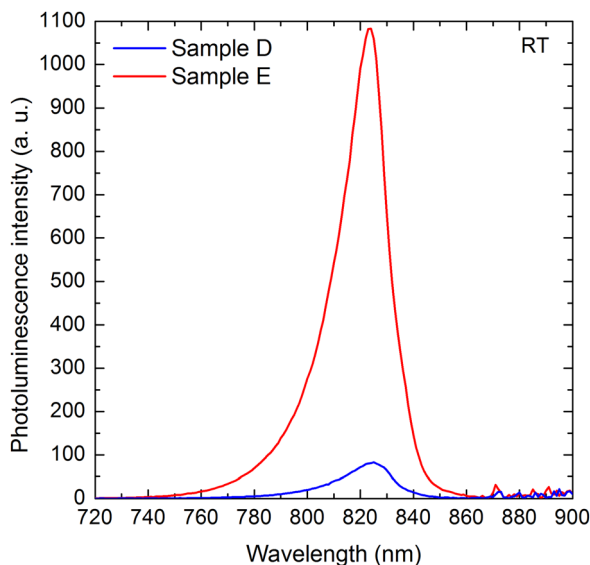

FIG. 4. (Color online) Room temperature photoluminescence spectra of samples D and E, showing that the integrated photoluminescence intensity of the CdZnTe/MgCdTe DH is over one order of magnitude stronger than that of the CdTe/MgCdTe DH.
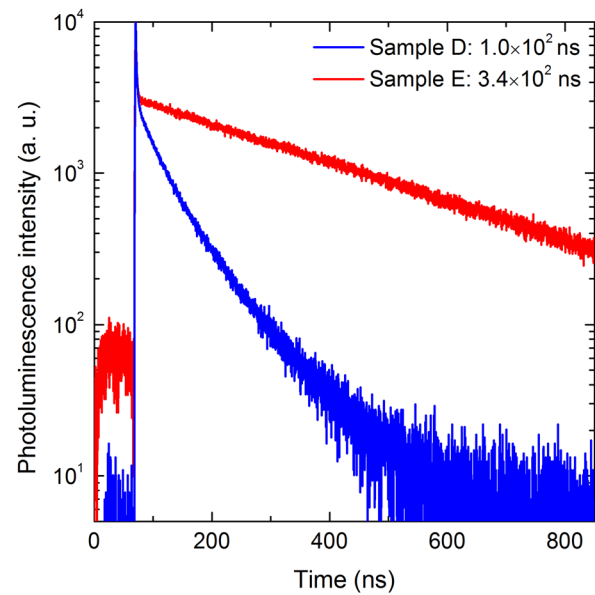

FIG. 5. (Color online) Time-resolved photoluminescence decays of samples D and E at room temperature, showing a significantly improved minority carrier lifetime, achieved by replacing CdTe with lattice-matched CdZnTe in the 3 μm DH design. The longest lifetime of 3.4×10^2 ns is observed.

and InSb is only 0.03%, the optical properties of the CdTe layer degrade noticeably due to the large density of misfit dislocations generated as a result of strain relaxation.

Figure 5 shows the room temperature PL decays of samples D and E measured by a time-correlated single photon counting system. The samples are excited by an ultrafast Ti:Sapphire laser with a 750 nm emission wavelength, a 130 fs pulse duration, and a 0.8 MHz repetition rate. The luminescence signal is detected by a spectrometer equipped with a high-speed microchannel plate photomultiplier tube, with the detection wavelength set at 820 nm. The minority carrier lifetimes of both samples are determined by fitting the tails of the decay curves, and are listed in Fig. 5. Sample E has a much longer measured lifetime (3.4×10^2 ns) than that of sample D (1.0×10^2 ns), which again proves the necessity of the lattice match to maintain low defect density and long carrier lifetime for a thick epilayer. Table I summarizes the strain relaxations, XRD FWHMs, integrated PL intensities and minority carrier lifetimes of samples D and E. These findings consistently prove that better structural and optical qualities are obtained in lattice-matched CdZnTe as opposed to CdTe grown on InSb substrates.

TABLE I. Strain relaxations, XRD FWHMs, integrated PL intensities, and minority carrier lifetimes of sample D: CdTe/MgCdTe DH, and sample E: CdZnTe/MgCdTe DH.

Sample	D	E
Strain relaxation in Cd(Zn)Te layer (%)	30	0
XRD FWHM of Cd(Zn)Te layer (arc sec)	22.6	16.6
Integrated PL intensity (a.u.)	2556	29717
Carrier lifetime (ns)	1.0×10^2	3.4×10^2

JVST B - Nanotechnology and Microelectronics: Materials, Processing, Measurement, and Phenomena

IV. SUMMARY

In summary, a CdZnTe ternary alloy completely lattice-matched to an InSb substrate has been demonstrated with accurate composition control using MBE. The Zn composition is determined to be 0.54% using XRD. Structural and optical properties comparisons have been carried out for 3 μm CdTe/MgCdTe DH and CdZnTe/MgCdTe DH samples grown on InSb substrates. Despite the fact that the lattice mismatch between CdTe and InSb is only 0.03%, the 3 μm CdTe layer has a relaxation of ∼30%, and its (004) XRD peak is wider than that of a 3 μm lattice-matched CdZnTe layer. It has also been observed that the CdZnTe/MgCdTe DH sample shows an integrated PL intensity one order of magnitude higher than, and a carrier lifetime three times as long as, those of the CdTe/MgCdTe DH sample. The longest carrier lifetime is measured as 3.4×10^2 ns for the CdZnTe/MgCdTe DH. These comparisons show the excellent material quality of a lattice-matched CdZnTe alloy grown on an InSb substrate, and manifest its great potential in high-efficiency solar cells and large-area focal plane arrays.

ACKNOWLEDGMENTS

[1]First Solar press release, 5 Aug 2014. First Solar achieves world's highest CdTe solar cell efficiency of 21.0%, see http://investor.firstsolar.com/releasedetail.cfm?ReleaseID=864426.

[2]T. A. Gessert *et al.*, Sol. Energy Mater. Sol. Cells **119**, 149 (2013).

[3]M. J. DiNezza, X.-H. Zhao, S. Liu, A. P. Kirk, and Y.-H. Zhang, Appl. Phys. Lett. **103**, 193901 (2013).

[4]A. P. Kirk, M. J. DiNezza, S. Liu, X.-H. Zhao, and Y.-H. Zhang, *Proceedings of the 39th IEEE Photovoltaic Specialists Conference*, Tampa, FL, 16–21 June 2013, pp. 2512–2517.

[5]X.-H. Zhao, M. J. DiNezza, S. Liu, S. Lin, Y. Zhao, and Y.-H. Zhang, J. Vac. Sci. Technol., B **32**, 040601 (2014).

[6]X.-H. Zhao, M. J. DiNezza, S. Liu, C. Campbell, Y. Zhao, and Y.-H. Zhang, Appl. Phys. Lett. **105**, 252101 (2014).

[7]D. Kuciauskas, A. Kanevce, J. M. Burst, J. N. Duenow, R. Dhere, D. S. Albin, D. H. Levi, and R. K. Ahrenkiel, IEEE J. Photovoltaics **3**, 1319 (2013).

[8]D. Kuciauskas, A. Kanevce, P. Dippo, S. Seyedmohammadi, and R. Malik, IEEE J. Photovoltaics **5**, 366 (2014).

[9]J. N. Duenow, J. M. Burst, D. S. Albin, D. Kuciauskas, S. W. Johnston, R. C. Reedy, and W. K. Metzger, Appl. Phys. Lett. **105**, 053903 (2014).

[10]A. Rogalski, Rep. Prog. Phys. **68**, 2267 (2005).

[11]O. Gravarnd *et al.*, J. Electron. Mater. **42**, 3349 (2013).

[12]R. Sporken, S. Sivananthan, K. K. Mahavadi, G. Monfroy, M. Boukerche, and J. P. Faurie, Appl. Phys. Lett. **55**, 1879 (1989).

[13]J. P. Zanatta *et al.*, J. Electron. Mater. **35**, 1231 (2006).

[14]R. N. Jacobs *et al.*, J. Electron. Mater. **41**, 2707 (2012).

[15]W. Lei, R. J. Gu, J. Antoszewski, J. Dell, and L. Faraone, J. Electron. Mater. **43**, 2788 (2014).

[16]T. J. de Lyon *et al.*, J. Electron. Mater. **39**, 1058 (2010).

[17]S. Adachi, *Handbook on Physical Properties of Semiconductors*, II-VI Compound Semiconductors (Kluwer Academic, Boston, MA, 2004), Vol. III, pp. 212 and 360.